LETTER

doi:10.1038/nature10353

Mutations in *UBQLN2* cause dominant X-linked juvenile and adult-onset ALS and ALS/dementia

Han-Xiang Deng[1]*, Wenjie Chen[1]*, Seong-Tshool Hong[1]†, Kym M. Boycott[2], George H. Gorrie[1]†, Nailah Siddique[1], Yi Yang[1], Faisal Fecto[1,3], Yong Shi[1], Hong Zhai[1], Hujun Jiang[1]†, Makito Hirano[1]†, Evadnie Rampersaud[4], Gerard H. Jansen[5], Sandra Donkervoort[1], Eileen H. Bigio[6], Benjamin R. Brooks[7], Kaouther Ajroud[1], Robert L. Sufit[1], Jonathan L. Haines[8], Enrico Mugnaini[3,9], Margaret A. Pericak-Vance[4] & Teepu Siddique[1,3,9]

Amyotrophic lateral sclerosis (ALS) is a paralytic and usually fatal disorder caused by motor-neuron degeneration in the brain and spinal cord. Most cases of ALS are sporadic but about 5–10% are familial. Mutations in superoxide dismutase 1 (*SOD1*)[1,2], TAR DNA-binding protein (*TARDBP*, also known as *TDP43*)[3,4] and fused in sarcoma (*FUS*, also known as translocated in liposarcoma (*TLS*))[5,6] account for approximately 30% of classic familial ALS. Mutations in several other genes have also been reported as rare causes of ALS or ALS-like syndromes[7–15]. The causes of the remaining cases of familial ALS and of the vast majority of sporadic ALS are unknown. Despite extensive studies of previously identified ALS-causing genes, the pathogenic mechanism underlying motor-neuron degeneration in ALS remains largely obscure. Dementia, usually of the frontotemporal lobar type, may occur in some ALS cases. It is unclear whether ALS and dementia share common aetiology and pathogenesis in ALS/dementia. Here we show that mutations in *UBQLN2*, which encodes the ubiquitin-like protein ubiquilin 2, cause dominantly inherited, chromosome-X-linked ALS and ALS/dementia. We describe novel ubiquilin 2 pathology in the spinal cords of ALS cases and in the brains of ALS/dementia cases with or without *UBQLN2* mutations. Ubiquilin 2 is a member of the ubiquilin family, which regulates the degradation of ubiquitinated proteins. Functional analysis showed that mutations in *UBQLN2* lead to an impairment of protein degradation. Therefore, our findings link abnormalities in ubiquilin 2 to defects in the protein degradation pathway, abnormal protein aggregation and neurodegeneration, indicating a common pathogenic mechanism that can be exploited for therapeutic intervention.

We identified a five-generation family (family 186) with ALS, including 19 affected individuals (Supplementary Information). The disease is transmitted in a dominant fashion with reduced penetrance in females. Mutations in the known ALS-linked genes were excluded. No evidence of genetic linkage was found with a genome-wide set of autosomal microsatellite markers. There was no evidence for male-to-male transmission of the disease, so we screened the family with markers from the X chromosome. Linkage was established with several microsatellite markers on the X chromosome, with the highest two-point lod score of 5.0 occurring with marker DXS9736 at $\Theta = 0$ (Supplementary Table 1). Detailed mapping with dense microsatellite markers and Illumina's Sentrix HumanHap300 Genotyping BeadChip defined the disease-causing gene in a 21.3-megabase (Mb) minimum candidate region (MCR) between markers rs6417786 and DXS1275, located in the pericentric region from Xp11.23 to Xq13.1.

No other large ALS families without male-to-male transmission were available to us to narrow down the MCR. We therefore focused on finding the causative gene in family 186. Of the 206 genes in this MCR, 191 were protein-coding. Genes in the MCR were analysed on the basis of their expression profile, function, structure and the potential relevance of their encoded proteins to disease. Forty-one genes were sequenced and a unique mutation in *UBQLN2* was identified. This mutation, a C to A substitution at position 1,490 at the level of coding DNA (c.1490C>A), is predicted to result in an amino-acid substitution of proline with histidine at codon 497 at the protein level (p.P497H) (Fig. 1a). The c.1490 C>A mutation co-segregated with the disease in this large X-linked-ALS pedigree (Fig. 1a). This mutation was not present in the SNP database, nor was it present in 928 ethnically matched control samples (representing 1,332 X chromosomes).

UBQLN2 is an intronless gene. To test whether mutations of *UBQLN2* are causative for other ALS patients, we analysed 188 probands from families with ALS or ALS/dementia, but without male-to-male transmission. Mutations in *SOD1*, *TDP43* and *FUS* were excluded in this cohort. The sequenced region covered the entire coding sequence (see Methods). We found four other *UBQLN2* mutations in four unrelated families, including c.1489 C>T (p.P497S), c.1516 C>A (p.P506T), c.1525 C>T (p.P509S) and c.1573 C>T (p.P525S) (Fig. 1 and Supplementary Fig. 1). All the amino-acid residues at the mutated sites are conserved (Fig. 1c). None of these mutations was present in the SNP database or in 928 control samples. Notably, all five ALS-linked *UBQLN2* mutations identified in this study involved proline residues in a unique PXX repeat region (Fig. 1c, d).

Clinical data were obtained from 40 individuals in the five families with *UBQLN2* mutations, including 35 patients and five obligate carriers. We estimated a penetrance of approximately 90% by the age of 70 years. The age of onset of the disease ranged from 16 to 71 years. A significant difference in age at onset was noted between male and female patients, with male patients having an earlier age of onset (33.9 ± 14.0 versus 47.3 ± 10.8 years, $P = 0.003$, two-tailed Student's *t*-test) (Supplementary Table 2). However, differences in the duration of the disease were not statistically significant (43.1 ± 42.1 versus 48.5 ± 19.9 months, $P = 0.61$). Eight patients with both ALS and dementia were identified. Dementia in these patients was similar to the frontotemporal lobar

[1]Division of Neuromuscular Medicine, Davee Department of Neurology and Clinical Neurosciences, Northwestern University Feinberg School of Medicine, Chicago, Illinois 60611, USA. [2]Department of Pediatrics, University of Ottawa and Children's Hospital of Eastern Ontario Research Institute, Ottawa, Ontario K1H 8L1, Canada. [3]Interdepartmental Neuroscience Program, Northwestern University Feinberg School of Medicine, Chicago, Illinois 60611, USA. [4]John P. Hussman Institute for Human Genomics, University of Miami, Miller School of Medicine, Miami, Florida 33136, USA. [5]Division of Anatomic Pathology, The Ottawa Hospital, Ottawa, Ontario K1Y 4E9, Canada. [6]Division of Neuropathology, Department of Pathology, Northwestern University Feinberg School of Medicine, Chicago, Illinois 60611, USA. [7]Department of Neurology, Neuroscience and Spine Institute, Carolinas Medical Center, Charlotte, North Carolina 28207, USA. [8]Center for Human Genetics Research, Vanderbilt University, Nashville, Tennessee 37232, USA. [9]Department of Cell and Molecular Biology, Northwestern University Feinberg School of Medicine, Chicago, Illinois 60611, USA. †Present addresses: Laboratory of Genetics and Department of Microbiology, Chonbuk National University Medical School, Chonbuk 561-712, South Korea (S.-T.H.); Institute of Neurological Sciences, Southern General Hospital, Glasgow G51 4TF, UK (G.H.G.); Department of Health Sciences, National Natural Science Foundation of China, Beijing 100085, China (H.J.); Department of Neurology, Sakai Hospital Kinki University Faculty of Medicine, Osaka 590-0132, Japan (M.H.).
*These authors contributed equally to this work.

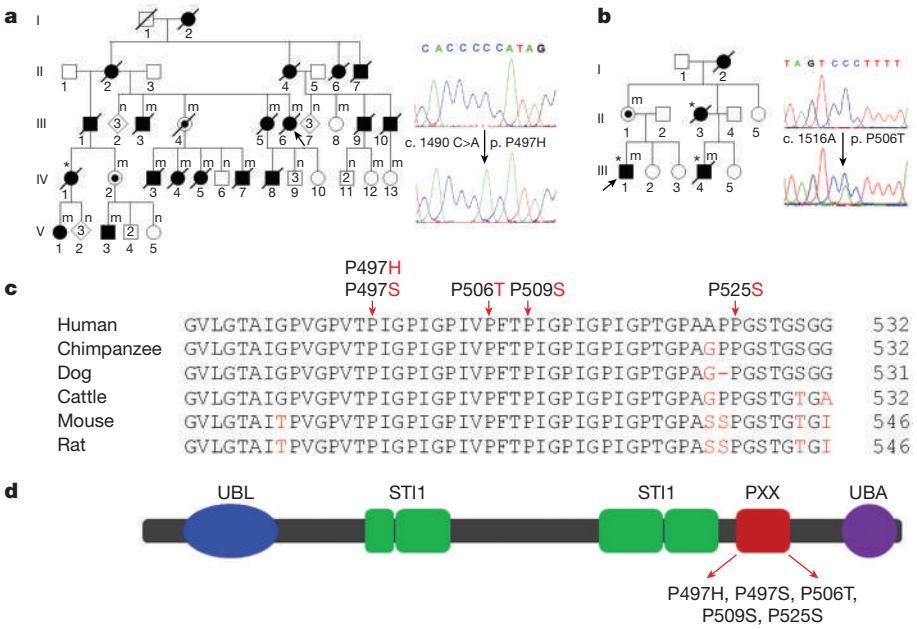

Figure 1 | Mutations of *UBQLN2* in patients with ALS and ALS/dementia. **a**, The mutation c.1490 C>A, resulting in p.P497H, was identified in a large family with ALS (family 186). This family was used to map X-linked ALS. The pedigree is shown on the left and DNA sequences are shown on the right: wild-type sequence (upper panel) and a representative hemizygous mutation in a male patient, V3 (lower panel). All affected members whose DNA samples were available for sequencing had the mutation. Two obligate carriers (III 4 and IV 2) were identified as having the same mutation. For simplicity and clarity, more than one unaffected individuals of both genders are represented by a single diamond and more than one unaffected male individual is represented by a single square. Filled symbols, affected individuals; open symbols, unaffected individuals; m, individuals with a mutation in *UBQLN2*; n, individuals without a mutation in *UBQLN2*. **b**, The mutation c.1516 C>A (p.P506T) was identified in family 6316: the pedigree is shown in the left panel and sequences in the right panel (showing a heterozygous mutation from a female obligate carrier, II 1). In **a** and **b**, probands are indicated with arrows and patients with dementia are indicated with asterisks. **c**, Evolutionary conservation of amino acids in the mutated region of ubiquilin 2 in various species. Comparison of human (*Homo sapiens*) ubiquilin 2 and its orthologues in chimpanzee (*Pan troglodytes*), dog (*Canis lupus familiaris*), cattle (*Bos taurus*), mouse (*Mus musculus*) and rat (*Rattus norvegicus*). Amino acids identical to those in the human protein are shown in black and non-identical ones are in red. The positions of the C-terminal amino acids are shown on the right. Mutated amino acids are indicated by arrows. **d**, Predicted structural and functional domains of ubiquilin 2, a protein of 624 amino acids. Predicted structural and functional domains include a ubiquitin-like domain (UBL, 33–103), four heat-shock-chaperonin-binding motifs (STI1), twelve PXX repeats (491–526) and a ubiquitin-associated domain (UBA). ALS- and ALS/dementia-linked mutations are clustered in the 12 PXX repeats.

type (FTD), including abnormalities in both behaviour and executive function. The dementia was progressive, and eventually global in most ALS/dementia patients. In some cases, the dementia preceded motor symptoms, but all patients eventually developed motor disability. Pathological analysis of spinal-cord autopsy samples from two patients with either the P497H or P506T mutation revealed axonal loss in the corticospinal tract, loss of anterior horn cells and astrocytosis in the anterior horn of the spinal cord (Supplementary Fig. 2).

Protein aggregates or inclusions have been recognized as a pathological hallmark of several neurodegenerative disorders, such as extracellular amyloid-β plaques and intracellular tau neurofibrillary tangles in Alzheimer's disease, and α-synuclein-containing Lewy bodies in Parkinson's disease[16]. In ALS, protein aggregates or inclusions are most common in spinal motor neurons, and are typically skein-like in morphology. These ubiquitin-positive inclusions, among others, are considered to be a hallmark of ALS pathology. Notably, several proteins that are mutated in a small subset of ALS, such as SOD1, TDP43, FUS and optineurin (OPTN) are prominent components of these inclusions[6,12,17–20]. To test whether ubiquilin 2 is present in the characteristic skein-like inclusions, we performed immunohistochemical analysis of post-mortem spinal-cord sections from two patients with a P497H or P506T mutation. Two different ubiquilin 2 antibodies were used. One was a commercially available mouse monoclonal antibody raised with a polypeptide of 71 amino acids from the carboxy terminus (amino acids 554–624, ubiquilin 2-C). The other was a rabbit polyclonal antibody that we generated using a polypeptide of 17 amino acids from the amino terminus (amino acids 8–24, ubiquilin 2-N). This polypeptide is unique to ubiquilin 2 and is not present in other members of the ubiquilin family or in any other known protein. The ubiquilin 2-N antibody immunoreacted with human and mouse ubiquilin 2 (Supplementary Fig. 3). We also detected a single band of the expected size in western blots using ubiquilin 2-N and ubiquilin 2-C antibodies with human spinal-cord autopsy tissues (Supplementary Fig. 3). Using immunohistochemistry, we saw skein-like inclusions that were immunoreactive with both the ubiquilin 2-C and ubiquilin 2-N antibodies (Supplementary Fig. 4), indicating that ubiquilin 2 is involved in inclusion formation in X-linked ALS. We then examined whether the inclusions in cases of X-linked ALS were also immunoreactive with antibodies against other proteins that are known to be involved in the formation of inclusions in other types of ALS. We found that the skein-like inclusions in the X-linked ALS patients were also immunoreactive with antibodies to ubiquitin, p62, TDP43, FUS and optineurin (Fig. 2a–c and Supplementary Figs 4 and 5), but not SOD1.

Mutations in TDP43, FUS or optineurin occur in a small fraction of familial ALS, but these proteins have been found in the inclusions of a wide spectrum of ALS[6,12,17,18,20]. To test whether ubiquilin 2 is involved in inclusion formation in other types of ALS, we examined 47 post-mortem spinal-cord samples, including cases of sporadic ALS ($n = 23$), familial ALS without mutations in *SOD1*, *TDP43* and *FUS* ($n = 5$), ALS with dementia ($n = 5$), familial ALS with *SOD1* mutations ($n = 7$ (A4V, $n = 4$; G85R, $n = 2$; E100G, $n = 1$)), familial ALS with a G298S mutation in *TDP43* ($n = 1$), and controls without ALS ($n = 6$). We observed ubiquilin-2-positive skein-like inclusions in all ALS cases (Supplementary Figs 6 and 7), indicating that ubiquilin 2 is a common component in the skein-like inclusions of a wide variety of ALS.

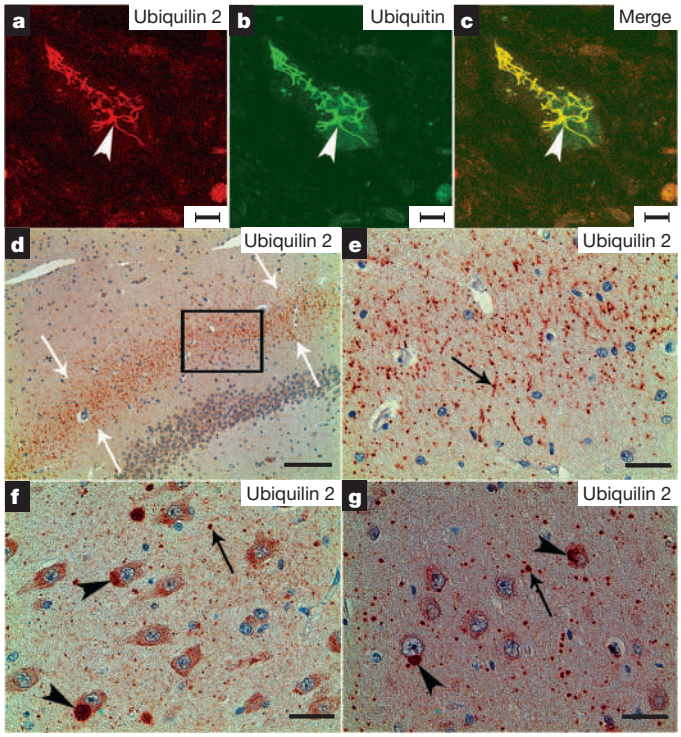

Figure 2 | Ubiquilin-2-immunoreactive inclusions in the spinal cord and hippocampus. **a**–**g**, Spinal cord (**a**–**c**) and hippocampal (**d**–**g**) sections from a patient with a UBQLN2^{P506T} mutation were analysed with confocal microscopy (**a**–**c**) and immunohistochemistry (**d**–**g**), using a monoclonal antibody against ubiquilin 2 (ubiquilin 2-C). The ubiquilin-2-positive and skein-like inclusions (arrowhead) are shown in a spinal motor neuron (**a**). These inclusions are also ubiquitin-positive (**b**, **c**). In the hippocampus, the ubiquilin-2-positive inclusions are shown in the molecular layer of the fascia dentata (**d**, **e**), CA3 (**f**) and CA1 (**g**). White arrows in **d** indicate the middle region of the molecular layer with ubiquilin-2-positive inclusions. A higher-magnification image of the boxed area in **d** is shown in **e**. Black arrows indicate representative inclusions in neurites (**e**–**g**), and arrowheads indicate cytoplasmic inclusions in the cell bodies (**f** and **g**). Scale bars: **a**–**c**, 10 μm; **d**, 200 μm; **e**, 50 μm; **f** and **g**, 25 μm.

Dementia was a prominent feature in eight *UBQLN2*-linked cases. To examine whether ubiquilin-2-immunoreactive inclusions are present in the brain, and to explore the potential link between ubiquilin 2 inclusions and dementia, we analysed brain autopsy samples from two patients with the P506T mutation. We saw ubiquilin 2 pathology, which was most prominent in the hippocampus (Fig. 2d–g and Supplementary Fig. 8). Small ubiquilin 2 inclusions (1–5 μm in diameter) were predominantly situated in the neuropil. The fascia dentata presented with a band of radially oriented dendritic and neuropil inclusions in the intermediate region of the molecular layer (Supplementary Fig. 8). In addition to the small neuropil inclusions, large inclusions (up to 20 μm in diameter) were observed in some pyramidal neurons, especially those in the CA3 and CA1 regions (Fig. 2f, g and Supplementary Fig. 8). Co-localization of ubiquilin 2 and ubiquitin in these inclusions was confirmed with confocal microscopy (Supplementary Fig. 8). This type of hippocampal pathology has not previously been observed in any other neurodegenerative disorder. The ubiquilin-2-positive and ubiquitin-positive inclusions did not seem to be co-localized with major glial markers (Supplementary Fig. 9). In addition, we observed a novel, membrane-bound perikaryal structure, which contained eosinophilic granules of varying sizes, in some hippocampal pyramidal neurons. These structures were strongly immunoreactive for ubiquilin 2 (Supplementary Fig. 10).

To test whether ubiquilin 2 pathology is present in the hippocampus of ALS/dementia cases without *UBQLN2* mutations, and to explore the correlation of ubiquilin 2 pathology with dementia in ALS, we examined hippocampal sections of 15 pathologically characterized ALS cases without *UBQLN2* mutations, including five cases of ALS/dementia with pathological signatures corresponding to frontotemporal lobar degeneration of motor-neuron-disease type (FTLD-MND/FTLD-U). We found prominent ubiquilin 2 pathology in the hippocampus of all five cases with ALS/dementia (Supplementary Fig. 11). Similar to the ubiquilin 2 inclusions in *UBQLN2*-linked ALS/dementia cases, the ubiquilin 2 inclusions in these non-*UBQLN2*-linked cases were also positive for ubiquitin and p62 (Supplementary Fig. 11), but negative for FUS. Although there was no apparent TDP43 neuritic pathology in the dentate molecular layer, we saw variable numbers of cytoplasmic TDP43 inclusions in dentate granule cells. These have previously been shown in ALS/dementia[18] (Supplementary Fig. 11). However, a notable number of the inclusions containing ubiquilin 2, ubiquitin and p62 were negative for TDP43 (Supplementary Figs 11 and 12). The absence of TDP43 in ubiquilin-2-positive inclusions was further confirmed with an antibody that specifically detects phosphorylated TDP43 in cytoplasmic TDP43 inclusions[18] (Supplementary Fig. 13). We also observed that the inclusions containing ubiquilin 2, ubiquitin and p62 were mostly negative for TDP43 in the CA regions in the non-*UBQLN2*-linked ALS/dementia cases (Supplementary Fig. 12). We did not observe ubiquilin 2 pathology in the hippocampus of the ten ALS cases without dementia. The correlation of hippocampal ubiquilin 2 pathology to dementia in ALS cases with or without *UBQLN2* mutations indicates that ubiquilin 2 is widely involved in ALS-related dementia, even without *UBQLN2* mutations.

TDP43 inclusions have been observed in dentate granule cells of the hippocampus in most cases with FTLD-U[18], and FUS inclusions have been shown in most TDP43-negative FTLD-U cases[21,22]. To test whether ubiquilin 2 co-aggregates with these two known ALS- and dementia-linked proteins *in vitro*, we generated ten expression constructs (Supplementary Information) and co-transfected Neuro-2a cells with different combinations of them. Both wild-type and mutant ubiquilin 2 were mostly distributed in the cytosol. We did not observe obvious differences in the distributions of wild-type and mutant ubiquilin 2. Wild-type FUS and wild-type TDP43 were located almost exclusively in the nuclei (Fig. 3 and Supplementary Fig. 14), whereas mutant FUS showed prominent cytoplasmic distribution (Supplementary Fig. 14) and the C-terminal fragment (218–414, C-TDP43) of TDP43 that has been linked to ALS and FTLD[18,23] was almost exclusively located in the cytosol (Fig. 3). We did not observe cytoplasmic inclusions in cells transfected with wild-type FUS and mutant FUS (Supplementary Fig. 14), nor with wild-type TDP43 (Fig. 3). However, cytoplasmic inclusions were seen in cells expressing either wild-type or mutant ubiquilin 2. Notably, C-TDP43 was co-localized with either wild-type or mutant ubiquilin 2 in the cytoplasmic inclusions (Fig. 3). We obtained consistent data using two expression systems: either tagged ubiquilin 2 or tag-free ubiquilin 2 (Fig. 3 and Supplementary Figs 14 and 15). These data indicate that both ALS- and dementia-linked ubiquilin 2 and TDP43 are prone to co-aggregation. We also noted that inclusion formation was apparently dose-dependent, because the cells with the lowest expression of wild-type or mutant ubiquilin 2, or C-TDP43, did not show cytoplasmic inclusions. However, ubiquilin-2-positive but C-TDP43-negative inclusions were frequently seen in cells with relatively lower levels of ubiquilin 2 and C-TDP43 expression (Fig. 3). This phenomenon indicates that ubiquilin 2 may be more prone to aggregation than TDP43. This is consistent with the pathology observed in ALS/dementia cases, in which the ubiquilin-2-containing inclusions in the molecular layer and in some dentate granule cells were TDP43-negative.

Ubiquilin 2 is a member of the ubiquitin-like protein family (ubiquilins). Humans have four ubiquilin genes, each encoding a separate protein. Ubiquilins are characterized by the presence of an N-terminal ubiquitin-like domain and a C-terminal ubiquitin-associated domain (Fig. 1d). The middle part of ubiquilins is highly variable. This structural organization is characteristic of proteins that deliver ubiquitinated

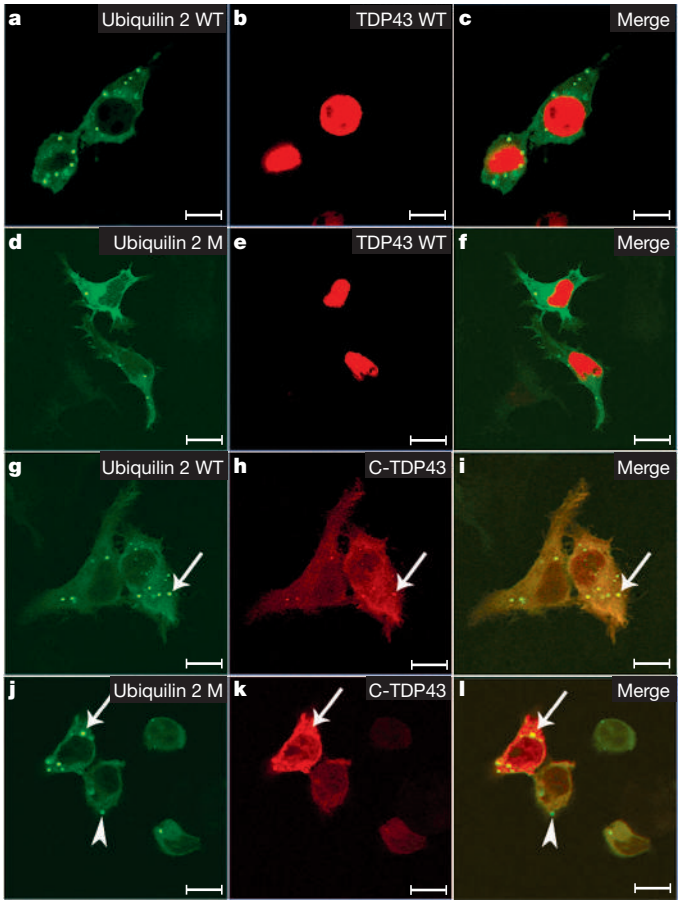

Figure 3 | Co-localization of ubiquilin 2 with ALS- and dementia-linked TDP43. a–l, Neuro-2a cells were transfected with various combinations of wild-type (WT) ubiquilin 2, mutant (M) ubiquilin 2 (P497H), wild-type TDP43 and a C-terminal fragment of TDP43 (amino acids 218–414) that is linked to ALS and FTLD. Ubiquilin 2 is GFP-tagged and TDP43 is mCherry-tagged. Wild-type and mutant ubiquilin 2 are mostly cytoplasmic. Wild-type TDP43 is located almost exclusively in the nuclei and C-TDP43 is almost exclusively cytoplasmic. TDP43 inclusions are co-localized with wild-type (**g–i**) and mutant (P497H) (**j–l**) ubiquilin 2 (arrows). Some ubiquilin-2-positive inclusions are TDP43-negative (arrowhead). Scale bars, 10 μm.

proteins to the proteasome for degradation. In accordance with this function, the ubiquitin-like domain of the ubiquilins binds to subunits of the proteasome, and the ubiquitin-associated domain binds to poly-ubiquitin chains that are typically conjugated onto proteins marked for degradation by the proteasome[24]. In addition to the ubiquitin-like and ubiquitin-associated domains that are shared by all ubiquilins, ubiquilin 2 has a unique repeat region containing 12 PXX tandem repeats (Fig. 1d). Notably, all five ALS-linked mutations identified in this study involve proline residues in this short PXX repeat region (Fig. 1c, d), indicating that these mutations may confer on ubiquilin 2 a common property that may be related to the pathogenic mechanism of the disease.

On the basis of the involvement of ubiquilin 2 in the protein degradation pathway, we then investigated the functional consequences of mutant ubiquilin 2 in protein degradation through the ubiquitin–proteasome system (UPS). We used a UPS reporter substrate, ubiquitin^{G76V} fused with green fluorescent protein (Ub^{G76V}–GFP)[25] to test the effects of mutant ubiquilin 2 on ubiquitin-mediated protein degradation. Two mutations at two different sites were tested (P497H and P506T) using the Ub^{G76V}–GFP reporter system. The G76V substitution prevents removal of N-terminally fused ubiquitin by cellular de-ubiquitinating enzymes, leading to efficient proteasomal degradation of the Ub^{G76V}–GFP reporter[25]. First, we tested the transfection efficiency of wild-type and mutant ubiquilin 2 constructs, and saw similar levels of exogenous ubiquilin 2 expression (Supplementary Fig. 16). We also tested the functionality of the Ub^{G76V}–GFP reporter system using the proteasome inhibitor MG-132 in transiently transfected cells. As expected, incubation with MG-132 resulted in marked accumulation of the Ub^{G76V}–GFP signal (Supplementary Fig. 17). We then examined the accumulation of Ub^{G76V}–GFP in Neuro-2a cells transiently transfected with either wild-type or mutant ubiquilin 2 constructs. Expression of mutant ubiquilin 2 resulted in significantly higher accumulation of Ub^{G76V}–GFP than expression of wild-type ubiquilin 2 (Fig. 4a). Similar data were obtained using SH-SY5Y cells (Supplementary Fig. 18).

We further analysed the dynamics of Ub^{G76V}–GFP degradation after new protein synthesis was blocked with cycloheximide for 0, 2, 4 and 6 h in Neuro-2a cells. We found that the rates of reporter degradation were significantly slower in cells expressing both the P497H and P506T ubiquilin 2 mutants, when compared to wild-type ubiquilin 2, at 4 h ($P < 0.05$) and 6 h ($P < 0.001$) (Fig. 4b), further supporting the notion that the ubiquilin 2 mutants impair the protein degradation pathway.

It is notable that all five ALS-linked *UBQLN2* mutations identified here involve four proline residues in the PXX region. Proline is a unique amino acid in that it has a side chain cyclized onto the backbone nitrogen atom, leading to steric restriction of its rotation, and thus hindering the formation of major known secondary structures. Moreover, among the primary structures of many ligands for protein–protein interactions, a proline residue is often critical[26]. Some protein–protein interaction domains, such as SH3, prefer ligand sequences containing tandem PXXP motifs, as noted in the PXX domain of ubiquilin 2, for high affinity and selectivity of such interactions[27]. Further studies of the consequences of the proline mutations may reveal interacting molecular partners that are relevant to the functions of ubiquilin 2.

The exact function of ubiquilin 2 is not well understood. However, there is increasing evidence that ubiquilins, together with their interactions with other proteins, may be involved in neurodegenerative disorders. Ubiquilin 1, another member of the ubiquilin family, is associated with Alzheimer's disease and interacts with presenilins 1 and 2 (ref. 28) and TDP43 (ref. 29). We observed that ubiquilin 2 formed cytoplasmic inclusions with ALS- and FTLD-linked TDP43, indicating that an interaction between TDP43 and ubiquilin 2 may underlie the pathogenesis of ALS and ALS/dementia, and possibly other neurodegenerative disorders as well.

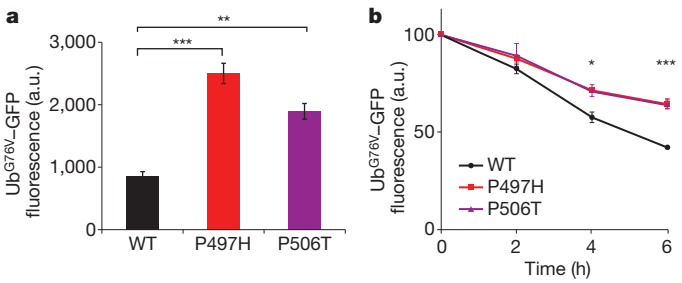

Figure 4 | Mutations in ubiquilin 2 lead to ubiquitin-mediated impairment of proteasomal degradation. a, b, Ub^{G76V}–GFP fluorescence intensity (arbitrary units, a.u.) was quantified by flow cytometry 48 h after transient transfection of Neuro-2a cells with either wild-type (WT) or mutant (P497H or P506T) *UBQLN2* (**a**). The dynamics of Ub^{G76V}–GFP reporter degradation after blockage of protein synthesis with cycloheximide for 0, 2, 4, and 6 h are shown in **b**. Rates of UPS-reporter degradation were significantly slower for both the P497H and P506T mutants when compared to the wild-type at 4 h and 6 h. Mean fluorescence before cycloheximide administration was standardized as 100%. Data are averaged from at least three independent experiments. *, $P < 0.05$; **, $P < 0.01$; ***, $P < 0.001$ (indicating significant differences when compared to wild-type by two-tailed Student's *t*-test). Error bars, means ± s.e.m.

The removal of misfolded or damaged proteins is critical for optimal cell functioning. In the cytosol and the nucleus, a major proteolytic pathway to recycle misfolded or damaged proteins is the UPS. Although an impaired UPS is thought to be associated with the formation of proteinaceous inclusions in many neurodegenerative disorders, direct evidence of mutations in the UPS pathway has been limited[30]. In this study, we show mutations of ubiquilin 2, a ubiquitin-like protein, in five families with ALS and ALS/dementia. We also show that inclusions containing ubiquilin 2 are a common pathological feature in a wide spectrum of ALS and ALS/dementia. Functional studies indicate an impairment of ubiquitin-mediated proteasomal degradation in cells expressing mutant ubiquilin 2. These data provide robust evidence for an impairment of protein turnover in the pathogenesis of ALS and ALS/dementia, and possibly in other neurodegenerative disorders as well. Further elucidation of these processes may be central to the understanding of pathogenic pathways. These pathways should provide novel molecular targets for the design of rational therapies for these disorders.

METHODS SUMMARY

Genomic DNA was PCR-amplified and Sanger-sequenced using a CEQ 8000 genetic analysis system (Beckman Coulter). Western blotting, immunohistochemistry and confocal microscopy were performed using previously established methods[17]. Construction of expression vectors, cell culture and flow cytometry were performed according to standard protocols. For statistical analysis, all graphs show mean ± s.e.m. and significance was calculated using Student's *t*-test.

Full Methods and any associated references are available in the online version of the paper at www.nature.com/nature.

Received 20 November 2010; accepted 5 July 2011.
Published online 21 August 2011.

1. Deng, H. X. *et al.* Amyotrophic lateral sclerosis and structural defects in Cu,Zn superoxide dismutase. *Science* **261,** 1047–1051 (1993).
2. Rosen, D. R. *et al.* Mutations in Cu/Zn superoxide dismutase gene are associated with familial amyotrophic lateral sclerosis. *Nature* **362,** 59–62 (1993).
3. Kabashi, E. *et al. TARDBP* mutations in individuals with sporadic and familial amyotrophic lateral sclerosis. *Nature Genet.* **40,** 572–574 (2008).
4. Sreedharan, J. *et al.* TDP-43 mutations in familial and sporadic amyotrophic lateral sclerosis. *Science* **319,** 1668–1672 (2008).
5. Kwiatkowski, T. J. Jr *et al.* Mutations in the *FUS/TLS* gene on chromosome 16 cause familial amyotrophic lateral sclerosis. *Science* **323,** 1205–1208 (2009).
6. Vance, C. *et al.* Mutations in FUS, an RNA processing protein, cause familial amyotrophic lateral sclerosis type 6. *Science* **323,** 1208–1211 (2009).
7. Chen, Y. Z. *et al.* DNA/RNA helicase gene mutations in a form of juvenile amyotrophic lateral sclerosis (ALS4). *Am. J. Hum. Genet.* **74,** 1128–1135 (2004).
8. Greenway, M. J. *et al. ANG* mutations segregate with familial and 'sporadic' amyotrophic lateral sclerosis. *Nature Genet.* **38,** 411–413 (2006).
9. Nishimura, A. L. *et al.* A mutation in the vesicle-trafficking protein VAPB causes late-onset spinal muscular atrophy and amyotrophic lateral sclerosis. *Am. J. Hum. Genet.* **75,** 822–831 (2004).
10. Yang, Y. *et al.* The gene encoding alsin, a protein with three guanine-nucleotide exchange factor domains, is mutated in a form of recessive amyotrophic lateral sclerosis. *Nature Genet.* **29,** 160–165 (2001).
11. Chow, C. Y. *et al.* Deleterious variants of *FIG4*, a phosphoinositide phosphatase, in patients with ALS. *Am. J. Hum. Genet.* **84,** 85–88 (2009).
12. Maruyama, H. *et al.* Mutations of optineurin in amyotrophic lateral sclerosis. *Nature* **465,** 223–226 (2010).
13. Ticozzi, N. *et al.* Paraoxonase gene mutations in amyotrophic lateral sclerosis. *Ann. Neurol.* **68,** 102–107 (2010).
14. Mitchell, J. *et al.* Familial amyotrophic lateral sclerosis is associated with a mutation in D-amino acid oxidase. *Proc. Natl Acad. Sci. USA* **107,** 7556–7561 (2010).
15. Johnson, J. O. *et al.* Exome sequencing reveals *VCP* mutations as a cause of familial ALS. *Neuron* **68,** 857–864 (2010).
16. Lansbury, P. T. & Lashuel, H. A. A century-old debate on protein aggregation and neurodegeneration enters the clinic. *Nature* **443,** 774–779 (2006).
17. Deng, H. X. *et al.* FUS-immunoreactive inclusions are a common feature in sporadic and non-SOD1 familial amyotrophic lateral sclerosis. *Ann. Neurol.* **67,** 739–748 (2010).
18. Neumann, M. *et al.* Ubiquitinated TDP-43 in frontotemporal lobar degeneration and amyotrophic lateral sclerosis. *Science* **314,** 130–133 (2006).
19. Shibata, N. *et al.* Intense superoxide dismutase-1 immunoreactivity in intracytoplasmic hyaline inclusions of familial amyotrophic lateral sclerosis with posterior column involvement. *J. Neuropathol. Exp. Neurol.* **55,** 481–490 (1996).
20. Mackenzie, I. R. *et al.* Pathological TDP-43 distinguishes sporadic amyotrophic lateral sclerosis from amyotrophic lateral sclerosis with *SOD1* mutations. *Ann. Neurol.* **61,** 427–434 (2007).
21. Neumann, M. *et al.* Frontotemporal lobar degeneration with FUS pathology. *Brain* **132,** 2922–2931 (2009).
22. Urwin, H. *et al.* FUS pathology defines the majority of tau- and TDP-43-negative frontotemporal lobar degeneration. *Acta Neuropathol.* **120,** 33–41 (2010).
23. Nonaka, T., Kametani, F., Arai, T., Akiyama, H. & Hasegawa, M. Truncation and pathogenic mutations facilitate the formation of intracellular aggregates of TDP-43. *Hum. Mol. Genet.* **18,** 3353–3364 (2009).
24. Ko, H. S., Uehara, T., Tsuruma, K. & Nomura, Y. Ubiquilin interacts with ubiquitylated proteins and proteasome through its ubiquitin-associated and ubiquitin-like domains. *FEBS Lett.* **566,** 110–114 (2004).
25. Dantuma, N. P., Lindsten, K., Glas, R., Jellne, M. & Masucci, M. G. Short-lived green fluorescent proteins for quantifying ubiquitin/proteasome-dependent proteolysis in living cells. *Nature Biotechnol.* **18,** 538–543 (2000).
26. Kay, B. K., Williamson, M. P. & Sudol, M. The importance of being proline: the interaction of proline-rich motifs in signaling proteins with their cognate domains. *FASEB J.* **14,** 231–241 (2000).
27. Aitio, O. *et al.* Recognition of tandem PxxP motifs as a unique Src homology 3-binding mode triggers pathogen-driven actin assembly. *Proc. Natl Acad. Sci. USA* **107,** 21743–21748 (2010).
28. Haapasalo, A. *et al.* Emerging role of Alzheimer's disease-associated ubiquilin-1 in protein aggregation. *Biochem. Soc. Trans.* **38,** 150–155 (2010).
29. Kim, S. H. *et al.* Potentiation of amyotrophic lateral sclerosis (ALS)-associated TDP-43 aggregation by the proteasome-targeting factor, ubiquilin 1. *J. Biol. Chem.* **284,** 8083–8092 (2009).
30. Aguzzi, A. & O'Connor, T. Protein aggregation diseases: pathogenicity and therapeutic perspectives. *Nature Rev. Drug Discov.* **9,** 237–248 (2010).

Supplementary Information is linked to the online version of the paper at www.nature.com/nature.

Acknowledgements This study was supported by the National Institute of Neurological Disorders and Stroke (NS050641), the Les Turner ALS Foundation, the Vena E. Schaff ALS Research Fund, the Harold Post Research Professorship, the Herbert and Florence C. Wenske Foundation, the David C. Asselin MD Memorial Fund, the Help America Foundation and the Les Turner ALS Foundation/Herbert C. Wenske Foundation Professorship. F.F. has support from NIH (T32 AG20506). K.A. is a postdoctoral fellow of the Blazeman Foundation for ALS. G.H.G. received travel funds from MND Scotland. We thank N. Dantuma for the UPS reporter plasmid (through Addgene) and the staff of the Northwestern University Robert H. Lurie Comprehensive Cancer Center flow cytometry core facility for technical assistance. Imaging work was performed at the Northwestern University Cell Imaging Facility, supported by NCI CCSG P30 CA060553 awarded to the Robert H Lurie Comprehensive Cancer Center.

Author Contributions T.S. conceived and supervised this project. W.C., S.-T.H., Y.Y., H.J., M.H., H.-X.D. and T.S. did the sequencing analysis. S.T.H., E.R., J.L.H., M.P.-V. and T.S. performed linkage analysis. K.M.B., G.H.G., F.F., G.H.J., H.Z., E.H.B., K.A., E.M., H.-X.D. and T.S. performed immunohistochemical, confocal and pathological analysis. F.F., Y.S. and H.-X.D. performed functional analysis. N.S., S.D. and T.S. collected family information and coordinated this study. K.M.B., G.H.J., B.R.B., R.L.S. and T.S. did clinical studies. H.-X.D. and T.S. analysed the data and wrote the paper.

Author Information Reprints and permissions information is available at www.nature.com/reprints. The authors declare no competing financial interests. Readers are welcome to comment on the online version of this article at www.nature.com/nature. Correspondence and requests for materials should be addressed to T.S. (t-siddique@northwestern.edu).

METHODS

Patients and samples. This study was approved by the local institutional review boards. ALS patients met the diagnosis of probable or definite ALS as defined in the revised EL-Escorial[31]. Patients with dementia met the criteria for FTD or FTLD proposed in refs 32 and 33. The dementia was similar to frontal variant FTD on inception and was progressive, and eventually global in most patients. One patient had mild mental retardation before the onset of dementia. There were eight patients with both ALS and dementia. Dementia preceded motor symptoms in some patients, but no patient remained free of motor involvement. The FTLD symptoms included abnormalities in both behaviour and executive function, although the degree of severity varied between individuals in different stages of the disease. Pedigrees and clinical data were collected by specialists in neuromuscular medicine and were verified by medical records or recent examination to establish diagnosis (Supplementary Table 2). DNA and other samples were taken after obtaining written informed consent. Overall, DNA from more than 200 ALS cases and 928 controls was used for genetic analysis. Spinal-cord autopsy samples from two X-linked ALS cases (P497H or P506T), 41 cases with ALS or ALS/dementia and six non-ALS controls were studied. In addition, available autopsy samples from the motor-cortex region of a patient with the P497H mutation (family 186, IV 7), brain regions (including hippocampus, cerebellum, optic nerve, visual cortex, pons and midbrain) of two patients with the P506T mutation (family 6316, II 3 and III 4), and the hippocampal regions of ten ALS and five ALS/dementia cases were also used for pathological and immunohistological studies. These five ALS/dementia cases were classified as having FTLD-MND/FTLD-U, including four cases with pathological type 3 and one case with pathological type 2 according to the classification system proposed in ref. 34. These cases were evaluated by a neuropathologist (E.H.B.).

Genetic analysis. Genomic DNA was extracted by standard methods (Qiagen) from whole peripheral blood, transformed lymphoblastoid cell lines or tissues. Intronic primers flanking exons were designed at least 50 nucleotides away from the intron/exon boundary. When a PCR product was larger than 500 base pairs (bp), several overlapping primers were designed with an average of 50-bp overlap. Genomic DNA (40 ng) was used for PCR amplification. The amplification protocol consisted of the following steps: incubation at 95 °C for 1 min, 32 cycles of 95 °C (30 s), 55 °C (30 s) and 72 °C (1 min), and a final 5-min extension at 72 °C, with modifications when necessary. Excess dNTPs and primers were digested with exonuclease I and shrimp alkaline phosphatase (ExoSAP-IT, USB). When non-specific PCR amplification occurred, the PCR products were separated on a 1.5% agarose gel and the specific PCR product was cut out from the gel and purified using QIAquick gel extraction kit (Qiagen). For sequencing of a PCR product, fluorescent-dye-labelled single-stranded DNA was amplified using Beckman Coulter sequencing reagents (GenomeLab DTCS quick start kit), followed by single-pass bidirectional sequencing with a CEQ 8000 genetic analysis system (Beckman Coulter). We sequenced the entire protein-coding exons and intronic sequences of 30–50 bp flanking the exons. *UBQLN2* is an intronless gene. We divided the *UBQLN2* gene into five overlapping PCR fragments for sequencing analysis. These fragments cover the entire coding sequence (1,872 bp), 125 bp of the 5′ UTR and 293 bp of the 3′ UTR. Primers were as follows: Ubqln2-1F, 5′-cttcatcacagaggtaccgtg-3′; Ubqln2-1R, 5′-gtgtggagttactcctgggag-3′; Ubqln2-2F, 5′-catgatgggctgactgttcac-3′; Ubqln2-2R, 5′-ctcttgtgcggcattcagcatc-3′; Ubqln2-3F, 5′-gacctggctcttagcaatctag-3′; Ubqln2-3R, 5′-gtgtctggattctgcatctgc-3′; Ubqln2-4F, 5′-cacagatgatgctgaatagcc-3′; Ubqln2-4R, 5′-gctgaatgaactgctggttgg-3′; Ubqln2-5F, 5′-ctgcacctagtgaaaccacgag-3′; Ubqln2-5R, 5′-aacagcattgattcccaccac-3′. For fragments 4 and 5, the PCR protocol consisted of the following steps: incubation at 96 °C for 2 min, 32 cycles of 96 °C (30 s), 56 °C (30 s) and 72 °C (1 min), and a final 5-min extension at 72 °C. The PCR products were separated on a 1.5% agarose gel and purified with QIAquick gel extraction kit (Qiagen) before sequencing.

Antibodies. Two anti-ubiquilin 2 antibodies were used. One was a mouse monoclonal antibody (5F5, H00029978-M03, Novus Biologicals Inc.). We made the other antibody, which was raised in rabbit using a polypeptide of human ubiquilin 2 (amino acids 8–24, SGPPRPSRGPAAAQGSA). The antiserum was affinity-purified. Other polyclonal and monoclonal antibodies used in this study included: anti-ubiquitin (PRB-268C, Covance; 10R-U101b, Fitzgerald Industries International; Ub(N-19):sc-6085, Santa Cruz Biotechnology), anti-p62 (H00008878-M01, Abnova; NB110-74805, Novus Biologicals Inc.), anti-TDP43 (TIP-PTD-P01, Cosmo Bio Co; 10782-2-AP, ProteinTech Group; 60019-2-Ig, ProteinTech Group; WH0023435M1-100UG, Sigma-Aldrich), anti-FUS (11570-1-AP, ProteinTech Group), anti-optineurin (100000, Cayman), anti-SOD1 (ref. 35), anti-Myc (MMS-150P, Covance), anti-GFAP (Z0334, Dako North America; G3893, Sigma-Aldrich), anti-Iba1 (019-19741, Wako Pure Chemical Industries) and anti-CNPase (MAB326R, Millipore).

Immunohistochemistry and confocal microscopy. The basic protocols for immunohistochemistry and confocal microscopy have been described in detail in a previous study[17]. In brief, 6-μm sections were cut from formalin-fixed, paraffin-embedded spinal cord and brain regions containing the frontal lobe or the hippocampus. The sections were deparaffinized with xylene and rehydrated with a descending series of diluted ethanol and water. Antigens in the sections were retrieved using a high-pressure decloaking chamber. For immunohistochemistry, endogenous peroxidase activity was blocked with 2% hydrogen peroxide. Non-specific background was blocked with 1% bovine serum albumin. The titres of the antibodies were determined on the basis of preliminary studies using serial dilution of the antibodies. Various antibodies against ubiquilin 2 or other proteins were used as primary antibodies. These included rabbit polyclonal anti-ubiquilin 2 (ubiquilin 2-N; 0.5 μg ml^{-1}; generated by us), mouse monoclonal anti-ubiquilin 2 (ubiquilin 2-C; 0.2 μg ml^{-1}; H00029978-M03, Novus Biologicals), rabbit polyclonal anti-FUS (3 μg ml^{-1}; 11570-1-AP, ProteinTech Group), mouse monoclonal anti-TDP43 (1 μg ml^{-1}; 60019-2-Ig, ProteinTech Group), rabbit polyclonal anti-TDP43 (0.1 μg ml^{-1}; 10782-2-AP, ProteinTech Group), mouse monoclonal anti-ubiquitin (0.5 μg ml^{-1}; 10R-U101B, Fitzgerald Industries International), rabbit polyclonal anti-ubiquitin (0.5 μg ml^{-1}; PRB-268C, Covance), goat polyclonal anti-ubiquitin (0.5 μg ml^{-1}; Ub(N-19):sc-6085, Santa Cruz Biotechnology), mouse monoclonal anti-p62 (1 μg ml^{-1}; H00008878-M01, Abnova Corporation) and rabbit polyclonal anti-optineurin (C-term; 0.2 μg ml^{-1}; 100000, Cayman). Biotinylated goat anti-rabbit and anti-mouse IgG, biotinylated mouse anti-goat IgG, or biotinylated rabbit anti-mouse IgG were used as the secondary antibodies. Immunoreactive signals were detected with peroxidase-conjugated streptavidin (BioGenex) using 3-amino-9-ethylcarbazole as a chromogen. The slides were counterstained with haematoxylin and sealed with Aqua PolyMount (Polyscience).

For confocal microscopy, antibodies generated in different species were used in various combinations. These antibodies included those against ubiquilin 2, FUS, TDP43, p62, optineurin, ubiquitin, Myc, GFAP, Iba1 and CNPase. Fluorescence signals were detected with appropriate secondary anti-rabbit, anti-mouse or anti-goat IgG, conjugated with Alexa Fluor 488 or Alexa Fluor 555 (Invitrogen), using an LSM 510 META laser-scanning confocal microscope with the multi-tracking setting[17]. The same pinhole diameter was used to acquire each channel.

Western blotting. Western blotting was performed using the protocol previously described[17]. Briefly, cells or spinal-cord tissues from lumbar segments were processed and homogenized. Cell lysates or the supernatants of tissue homogenates were subjected to total protein quantification, gel electrophoresis and blotting on PVDF membranes. Ubiquilin 2 was detected using the ubiquilin 2-N or ubiquilin 2-C antibodies. The membranes were then stripped and blotted with an antibody against β-actin (A5441, Sigma-Aldrich).

Expression constructs. A full-length human cDNA clone (*Homo sapiens* ubiquilin 2, IMAGE:4543266) was used as a template for construction of the expression constructs. Two primers anchored with a XhoI site (ubiquilin 2-TP1, 5′-ttctcgaggg ccgccatggctgagaat-3′) and a BamHI site (ubiquilin2-TP2, 5′-catggatcctgtatgtctgt attacc-3′) were used to amplify the full-length coding sequence. The amplified fragment was cloned into plasmid vector pBluescript M13. The ubiquilin 2 sequence was verified by direct sequencing. The P497H and P506T mutations were introduced into the plasmid vector by site-directed mutagenesis using a primer containing each respective mutation. The XhoI/BamHI fragment containing wild-type *UBQLN2*, *UBQLN2*^{P497H} or *UBQLN2*^{P506T} was released from the pBluescript M13 vector and cloned into the XhoI and BamHI sites of dual expression vectors pIRES2-DsRed2 or pIRES2-ZsGreen1 (Clontech), to create such constructs as wtUBQLN2-ZsGreen1 and mUBQLN2-ZsGreen1 (mutant ubiquilin 2 (P497H or P506T)).

We generated seven additional expression constructs, including wild-type ubiquilin 2 tagged with GFP (wtUBQLN2–GFP), mutant ubiquilin 2 (P497H or P506T) tagged with GFP (mUBQLN2–GFP), wild-type TDP43 tagged with mCherry (wtTDP43–mCherry), an ALS- and dementia-linked C-terminal fragment of TDP43 (amino acids 218–414, C-TDP43)[18,23] tagged with mCherry (C-TDP43–mCherry), wild-type FUS tagged with Myc (Myc–wtFUS) and mutant FUS (R495X) tagged with Myc (Myc–mFUS).

Cell culture, transfection and immunocytochemistry. SH-SY5Y, Neuro-2a and HEK293 cell lines were grown on collagen-coated plates in Dulbecco's modified Eagle's medium containing 10% (v/v) human serum, 2 mM L-glutamine, 2 U ml^{-1} penicillin and 2 mg ml^{-1} streptomycin, at 37 °C in a humidity-controlled incubator with 5% CO_2. The cells were transiently transfected with different combinations of expression vectors using Lipofectamine 2000 (Invitrogen) according to manufacturer's instructions. Immunocytochemistry was performed as previously described[36].

UPS reporter assay. SH-SY5Y and Neuro-2a cells were grown in 24-well plates and double-transfected with a UPS-reporter vector encoding Ub^{G76V}–GFP (ref. 25) (Addgene plasmid 11941), and a dual expression vector encoding DsRed2 with either wild-type or mutant ubiquilin 2. Cells were harvested 48 h after transfection and resuspended in PBS. Cells transfected with the Ub^{G76V}–GFP vector were used for control experiments to test the functionality of the UPS reporter. In these control experiments, the medium was changed 24 h after

transfection to medium containing 5 μM proteasomal inhibitor MG-132 (A.G. Scientific Inc.). Cells were incubated in this medium for 24 h and then harvested and resuspended in PBS. For cycloheximide chase of UB^{G76V}–GFP, transiently transfected Neuro-2a cells were used. The cells were transferred 24 h after transfection to medium containing 5 μM MG-132. After incubation with MG-132 for 16 h to accumulate the Ub^{G76V}–GFP reporter, cells were washed in sterile PBS and incubated with medium containing 100 μg ml^{-1} cycloheximide (Sigma) for 0, 2, 4, and 6 h. At each time point, cells were washed, harvested and resuspended in ice-cold PBS supplemented with 100 μg ml^{-1} cycloheximide. The fluorescence intensities at each time point were measured by flow cytometry. The fluorescence intensity at 0 h was taken to be maximal fluorescence (100%). All flow-cytometric data were collected and analysed using a MoFlo cell sorter and Summit software (DakoCytomation). Argon-ion (488 nm) and yellow (565 nm) lasers were used for excitation. The GFP and DsRed2 signals were collected using 530/540-nm and 600/630-nm bandpass filters, respectively. In all experiments, data were gated on GFP/DsRed2 dual-labelled cells. At least 500–1,000 such events were recorded in each experiment. The DsRed2 expression levels and profiles were similar across experiments. Data were collected from three independent experiments. Two-tailed unpaired Student's *t*-test ($P < 0.05$) was used for statistical analysis.

31. Brooks, B. R., Miller, R. G., Swash, M. & Munsat, T. L. El Escorial revisited: revised criteria for the diagnosis of amyotrophic lateral sclerosis. *Amyotroph. Lateral Scler. Other Motor Neuron Disord.* **1,** 293–299 (2000).
32. Neary, D. *et al.* Frontotemporal lobar degeneration: a consensus on clinical diagnostic criteria. *Neurology* **51,** 1546–1554 (1998).
33. Cairns, N. J. *et al.* Neuropathologic diagnostic and nosologic criteria for frontotemporal lobar degeneration: consensus of the consortium for frontotemporal lobar degeneration. *Acta Neuropathol.* **114,** 5–22 (2007).
34. Mackenzie, I. R. *et al.* Heterogeneity of ubiquitin pathology in frontotemporal lobar degeneration: classification and relation to clinical phenotype. *Acta Neuropathol.* **112,** 539–549 (2006).
35. Deng, H. X. *et al.* Conversion to the amyotrophic lateral sclerosis phenotype is associated with intermolecular linked insoluble aggregates of SOD1 in mitochondria. *Proc. Natl Acad. Sci. USA* **103,** 7142–7147 (2006).
36. Fecto, F. *et al.* Mutant TRPV4-mediated toxicity is linked to increased constitutive function in axonal neuropathies. *J. Biol. Chem.* **286,** 17281–17291 (2011).